WEP Warwick Evans Publishing

International Journal of Materials Science and Technology Studies

ISSN: 3006-7693 (Print), ISSN: 3006-3744 (Online) | Volume 3, Number 1, Year 2025
DOI: https://doi.org/10.62051/ijmsts.v3n1.08
Journal homepage: https://wepub.org/index.php/IJMSTS/index

Research on the Optimization of Optical Properties of Colorants for Plastics based on Multichannel Theory

Zijian Lin [1], Xinyu Lin [2], Xiaoyin Wang [2, *]

[1]School of Software, Tiangong University, Tianjin, China
[2]School of Textile Science and Engineering, Tiangong University, Tianjin, China
[*]Corresponding Author: Xiaoyin Wang (E-mail: wangxiaoyin@tiangong.edu.cn)

ABSTRACT

In the field of plastic color matching, the accuracy of color prediction directly affects the precise control of attributes such as hue, brightness, and saturation, thereby influencing the coloring effect of pigments. This paper conducts an in-depth study based on many-flux method and finite difference analysis, dividing the scattering medium into multiple light transmission channels according to the angle of light incidence. We investigate the flux transfer relationships between the channels to address the shortcomings of the Kubelka-Munk(K-M) theory in achieving satisfactory coloring effects in non-diffuse environments with weak scattering or thin media. Using polypropylene as the substrate, we analyze the optical properties of pigments under D65 light sources with a 10nm interval. Under conditions of higher transparency and lower scattering coefficients, we establish the relationship between the absorption coefficient K, scattering coefficient S, and reflectance R. Finally, we compare the experimental results with the reflectance errors of actual samples to optimize the theoretical model, thereby improving the coloring performance, by analyzing the K-M theory model and the multichannel model for high-concentration red pigment (DPP P.R.254) and high-concentration green pigment (Copper Phthalocyanine P.G.7).

KEYWORDS

Color matching; Plastic; Reflectance prediction; Finite difference method

1. INTRODUCTION

Color is an incredibly significant element in visual communication, through which information and emotions may be transmitted. And pigments may substantially enrich human's daily existence and increase the quality of life through their diverse hues and functions. Therefore, color science has been intensively investigated in numerous technical domains, notably in sectors such as textiles and plastics. With the growing demand for color and the continuous advancement of computer technology, the digital study of colour information is rapidly attracting substantial attention from technicians.

In the conventional production process, the colour mixing of pigments generally relies on manual experience, which is not only inefficient but also difficult to assure the accuracy and consistency of colours. However, with the introduction of computer technology, this scenario has been substantially improved. The use of advanced computer technology to accurately control the colour of pigments can realize the automation and intelligence of the production process. So that it can significantly improve production efficiency and, at the same time reduce the rate of scrap due to manual errors and the waste of raw materials. It can also optimize the production process and reduce unnecessary manpower

and material inputs. Thus, it can effectively save production costs and bring greater economic benefits to the enterprise.

Color variances between pigments primarily stem from the differences in their optical properties under visible light, where the color of a pigment is primarily determined by the medium's reflectance under different wavelengths of light. Furthermore, the multiple scattering and absorption of incident light inside the medium are important factors affecting the reflectance [1-4]. In pigment color matching, the K-M theory is typically used to calculate pigment reflectance. By measuring the scattering coefficient and absorption coefficient of pigments, the reflectance spectra of different pigment combinations at various ratios can be calculated, and the color of the mixing can then be determined. Since its proposal, the K-M theory has been subjected to numerous theoretical studies and practical verifications, and it has already gained a deep foundation of application and a wealth accumulation of experience in the field of pigment color matching. Despite its limitations, the accuracy can be improved to some extent by many correction methods proposed by previous authors[5][6]. However, the new parameters, variables, or coefficients introduced in the correction process complicate the original relatively simple K-M equations, increasing the difficulty and workload of the calculation and requiring a higher performance of the calculation equipment. Meanwhile, the correction is only carried out for specific pigment systems, application environments, or measurement conditions, which makes the corrected theory able to achieve better results under these specific conditions, but in other cases, it is not, which reduces the generality of the theory and prevents it from being widely used in a variety of different pigment matching scenarios. For the K-M optical model there are still many assumptions that cannot be corrected, Mudgett and Richard proposed a computational scheme based on multiple scattering, called the many-flux method. It can be extended to 16, 26, or even more channels compared to the K-M two-flux method and Beasley's four-flux method, which is essentially a generalization of the K-M two-flux method [7]. Despite the relative mathematical complexity of the many-flux method, its computational feasibility is verified.

The researches listed above are all based on color matching for opaque media. For plastic color matching, the K-M optical model is difficult to apply. Meanwhile, there is less research related to the many-flux method, and it is mostly concentrated in fields such as ink printing, etc. Nowadays, most of the research on plastic color matching uses cluster analysis, which requires a high demand for the data to be selected and the algorithms to be applied while also being difficult to comprehend and accept[8]. In this paper, we discretize and solve the phase function in Mie theory to compute scattered light intensity at any angle, and then utilize the finite difference method to solve the radiative transfer equation for numerous channels to determine each channel's luminous flux. Finally, a visual analysis is performed following sample testing, and it can be seen that the accuracy of the model in this paper is significantly improved when dealing with more transparent media than predicting reflectance curves using the absorption coefficient K and scattering coefficient S .

2. OPTICAL THEORY FOUNDATION AND MODELING

2.1. Mie Scattering Theory-based Radiative Transfer Equation

2.1.1. Scattering and Mie Scattering

A combination of an object's selective absorption, scattering, and reflection of light at various wavelengths determines its color[9]. Understanding how light scatters can help us better grasp how an object's color is formed. The ratio of the particle's diameter to the light wave's wavelength determines the scattering's direction and intensity. Different kinds of scattering processes, including Rayleigh scattering and Mie scattering, occur when the wavelength-to-particle size ratio changes. In general, the size of the scattering particles in plastics is equal to or greater than the incident light's wavelength, at which point Mie theory may adequately describe it. According to the Mie theory, when incident light is incident vertically, the forward scattering intensity along the incident direction is typically the

most significant. However, because of the medium or particles present, some light will also be scattered in other directions, but the intensity of the light exhibits rotational symmetry in the plane of incidence. Additionally, the distribution of scattered light intensity varies in each direction away from the angle of incidence.

The incident angle of the incoming direction is 0°, which means vertical incidence.θ is the angle of light scattering, then the dispersed light in the direction away from the angle θ of incidence can be expressed as follows:

$$I_\theta = \frac{N}{L^2}\left(\frac{\lambda_m}{2\pi}\right)\left(\frac{|S_1|^2 + |S_2|^2}{2}\right)I_0 \tag{1}$$

Where, I_0 is the incident light, λ_m is the wavelength of light in a medium whose refractive index is n_m, L is the distance between the test point and the scattering center, N is the number of particles per unit volume [10-11].

S_1 and S_2 are the amplitude functions of light with the expression:

$$\begin{cases} S_1 = \sum_{l=1}^{\infty} \frac{2l+1}{l(l+1)}[a_l \cdot \pi_l(\cos\theta) + b_l \cdot \tau_l(\cos\theta)] \\ S_2 = \sum_{l=1}^{\infty} \frac{2l+1}{l(l+1)}[a_l \cdot \tau_l(\cos\theta) + b_l \cdot \pi_l(\cos\theta)] \end{cases} \tag{2}$$

Where, a_l,b_l is the Mie coefficient.

$$\begin{cases} a_l = \frac{\psi_l(\alpha)\psi_l'(m\alpha) - m\psi_l'(\alpha)\psi_l(m\alpha)}{\zeta_l(\alpha)\psi_l'(m\alpha) - m\zeta_l'(\alpha)\psi_l(m\alpha)} \\ b_l = \frac{m\psi_l(\alpha)\psi_l'(m\alpha) - \psi_l'(\alpha)\psi_l(m\alpha)}{m\zeta_l(\alpha)\psi_l'(m\alpha) - \zeta_l'(\alpha)\psi_l(m\alpha)} \end{cases} \tag{3}$$

Where α is the particle size parameter, m is the particle's refractive index relative to the surrounding radius, and $m = m_1 + im_2$, where m_1 represents the real part (refractive index) and m_2 represents the imaginary part (absorptivity), if the latter is not zero, the particle is said to have absorptive properties. ψ_l and ζ_l are the combinations of the Bessel functions of the first kind of half-integer order and the Hankel functions of the second kind, respectively. The recurrence formulas are derived using the Legendre polynomials [12] with the recurrence relations of the Bessel and Hankel functions:

$$\begin{cases} \psi_l(\alpha) = \dfrac{2l-1}{\alpha}\psi_{l-1}(\alpha) - \psi_{l-2}(\alpha) \\ \zeta_l(\alpha) = \dfrac{2l-1}{\alpha}\zeta_{l-1}(\alpha) - \zeta_{l-2}(\alpha) \\ \psi_l'(\alpha) = \psi_{l-1}(\alpha) - \dfrac{l}{2}\psi_l(\alpha) \\ \zeta_l'(\alpha) = \zeta_{l-1}(\alpha) - \dfrac{l}{2}\zeta_l(\alpha) \end{cases} \tag{4}$$

The initial value is:

$$\begin{cases} \psi_0(\alpha) = \sin\alpha \\ \psi_1(\alpha) = \dfrac{1}{\alpha}\sin\alpha - \cos\alpha \\ \zeta_0(\alpha) = \sin\alpha + i\cos\alpha \\ \zeta_1(\alpha) = \dfrac{1}{\alpha}(\sin\alpha + i\cos\alpha) - (\cos\alpha - i\sin\alpha) \end{cases} \tag{5}$$

π and τ are determined by the loop functions listed below:

$$\begin{cases} \pi_l(\cos\theta) = \dfrac{2l-1}{l-1}\cos\theta \cdot \pi_{l-1}(\cos\theta) - \dfrac{l}{l-1}\pi_{l-2}(\cos\theta) \\ \tau_l(\cos\theta) = l\cos\theta \cdot \pi_l(\cos\theta) - (l-1)\pi_{l-1}(\cos\theta) \end{cases} \tag{6}$$

The loop function's initial function is:

$$\begin{cases} \pi_0(\cos\theta) = 0 \\ \pi_1(\cos\theta) = 1 \\ \pi_2(\cos\theta) = 3\cos\theta \\ \tau_1(\cos\theta) = \cos\theta \\ \tau_2(\cos\theta) = 3\cos 2\theta \end{cases} \tag{7}$$

All of the aforementioned loop functions have been shown to converge, making them suitable for use in streamlining computations.

2.1.2. Phase Function for Mie Scattering

Following the computation of (1) to determine the intensity of the scattered light at the scattering angle θ, greater emphasis should be placed on the characteristics of the light scattering distribution at various angles. To overcome the challenge of precisely representing the intensity distribution of light at different scattering angles, we introduce the scattering phase function $p(\theta)$ [18] to characterize the variation of this angular distribution. The phase function under Mie scattering may be written as follows:

$$p(\theta) = \frac{2(i_1 + i_2)}{Q_{sc}\alpha^2} \tag{8}$$

Where, i is the scattering intensity function, which can be further expressed by the amplitude function S and its conjugate complex, that is,$i = S \cdot S^*$. The scattering efficiency factor Q_{sc}[10] is associated with the scattering cross-section of the particles as well as the geometrical cross-section of the particles, which can calculated using:

$$Q_{sc}(\alpha, m) = \frac{2 \cdot \sum_{j=1}^{\infty} (2n+1)(|a_j|^2 + |b_j|^2)}{\alpha^2} \tag{9}$$

Where n is the radius of the particles.

2.1.3. Radiative Transfer Theory

On the basis that the phase function of Mie scattering accurately describes the change of scattered light intensity with the scattering angle, radiative transfer theory can further take into account the multiple light scattering of numerous particles as well as the process of multiple scattering of light in the medium, so as to more comprehensively describe the propagation and energy transfer of light in the medium.

The radiative transfer equation, which is the core of the theory, begins with the particle nature of light. It disregards the polarization and interference phenomena of light waves and only tracks the energy transfer of light in the medium while considering the intensity change of radiation under the influence of absorption and scattering [14]. When the medium's radiation is not taken into account, the one-dimensional radiative transfer equation is expressed as [11]:

$$\mu \frac{dI_d(\tau, \mu)}{d\tau} + I_d(\tau, \mu) = \frac{1}{2}\int_{-1}^{1} d\mu' P(\mu, \mu')\, I_d(\tau, \mu') \tag{10}$$

$$I_d(0, \mu) = a, (0 < \mu < 1) \tag{11}$$

$$I_d(d, \mu) = b, (-1 < \mu < 0) \tag{12}$$

Where, μ is the direction cosine, that is, $\mu = \cos\theta$, I_d represents the radiation intensity. τ is the radiation space between 0 and the medium's thickness d , indicating the optical depth of radiation transmission in the medium. $P(\mu, \mu')$ is the radiant luminance percentage scattered from the direction μ' to the direction μ . Equations (11) and (12) serving as boundary conditions together with Equation (10) constitute the complete radiation transfer equation. Assuming that when $\mu = 1$, the direction of light propagation is forward propagation, then a is the incident flux of light in the forward propagation, while b is the light flux when the light is transmitted to the back of the medium and then reflected back to the interior of the medium. In the radiative transfer equation, the intensity of radiation varies only with the optical distance τ and angle θ .

2.2. Multichannel Model

In order to more precisely characterize and quantify the energy flux reflected inside the medium, many-flux method is further introduced based on the theoretical framework mentioned above. This model calculates the energy transfer between channels.

The many-flux method is an extension of the K-M two-flux method. The two-flux method, which is the simplest form of the radiation transfer function, assumes that light is dispersed in just two directions and that the intensity of the scattered light is equal. Based on this, the many-flux method separates the angle between the incident and dispersed light into $2n$ groups, each of which corresponds to a channel. From the stereoscopic viewpoint, the i channel is between the solid angle θ_i and the solid angle θ_{i+1}. The angle between the first n channels and the incident angle is smaller than 90°, but the angle between the last n channels and the incident angle is larger than 90°. In addition, the angle between the i channel and the $2n-i$ channel is complementary. Compared with the K-M theory, the propagation directions represented by different channels are various in the many-flux method, with all rays within the same channel reaching the boundary of the scattering medium at approximately the same angle of incidence[7]. By solving the differential equations for radiative transfer, we may compute the radiant energy incident from any direction in many-flux method for 2n channels[15][16][17].

When the scattering medium's optical thickness is small, the polarization effect is more noticeable. We suppose that the optical thickness of the medium can experience repeated scattering, which would cause the polarized light to lose its original polarization state. This simplifies the model, allowing the polarized light to be disregarded and only the overall intensity of the scattered light to be estimated.[18]

3. ALGORITHM FOR SOLVING THE RADIATION EQUATION

3.1. Algorithm for Discretization of the Scattering Phase Function

On a spherical coordinate, the latitude of the sphere is denoted by the polar angle θ and the longitude of the sphere is denoted by the azimuthal angle φ, where $\theta \in (0,\pi), \varphi \in (0,2\pi)$. Assuming that the direction of incidence of a parallel beam of light is (0,0), when the light travels through the medium and Mie scattering takes place, the scattering intensity distribution in different directions can be found out through Equation (8), which is noted as $p(\theta,\varphi)$. If the azimuths of the two points (θ_1,φ_1) and (θ_2,φ_2) are equal, i.e.$\varphi_1 = \varphi_2$, then the scattered intensities of the two points are equal. The intensity distribution of the scattering, in this case, is independent of the azimuth φ, which can be simplified to $p(\theta)$. Assuming that the angle between any two points $a(\theta,\varphi)$ and $b(\theta',\varphi')$ in space is $(\theta,\varphi;\theta',\varphi')$, then the intensity of scattering from the direction where b is located to the direction where a is located is noted as $p(\theta,\varphi;\theta',\varphi')$.

The above is a description of the scattering intensity in the Mie theory in the form of coordinates. Both θ and φ must be considered in that description. If the azimuth φ is not taken into account, only the average value of the scattering of a point (θ',φ') to all the points on the latitude with a polar angle of θ is calculated:

$$p(\theta;\theta') = \int_0^{2\pi} p(\theta,\varphi;\theta',\varphi')d\varphi \tag{13}$$

Because of the symmetry of the azimuthal angles within the same channel, (13) can also represent the average intensity of scattering from all points on the latitude with the polar angle θ' to the latitude

with the polar angle θ. Going a step further, instead of using θ, the cosine value μ is used as the variable, then the proportion of scattering from one latitude interval $[a, b]$ to another latitude, accounting for all latitudes at this point, is:

$$P(\mu, \mu') = \frac{\int_{\cos(a)}^{\cos(b)} p(\mu; \mu') d\mu'}{\int_{-1}^{1} p(\mu) d\mu} \tag{14}$$

Where P is part of the integrand in (10). If the model is discretized at this point, dividing both the polar and azimuthal angles into an even number of discrete points, N and M respectively, so that $\mu = \{\mu_1, \mu_2, \ldots, \mu_N\}$ and $\varphi = \{\varphi_1, \varphi_2, \ldots, \varphi_M\}$. Combined with the many-flux method, each μ can be regarded as a channel F, then the contribution of the channel F_j scattering to F_i accounts for the contribution of all the channels scattering to F_i is :

$$P(\mu_i, \mu_j) = \frac{\sum_{k=1}^{M} p(\mu_i, \varphi_k; \mu_j, \varphi')}{M \sum_{k=1}^{N} p(\mu)} \tag{15}$$

Where, φ' can be any value from the set φ, P is the scattering phase function in the radiative transfer equation solved by the discrete method.

3.2. Finite Difference Method for Solving the Radiative Transfer Equation

By discretizing a continuous partial differential equation into a set of algebraic equations, the finite difference method is a numerical computing technique that makes partial differential equations numerically solvable. Meshing, approximating finite differences, substituting equations, solving algebraic equations, and applying starting and boundary conditions are some of the specific steps. Finally, an approximate solution can be obtained through iterative solving[19].

Since the radiative transfer equation is a differential integral equation, it is more difficult to solve directly. This paper approximates the integral in the equation using the summation function, which converts the differential integral equation into a differential equation and then solves the radiative transfer equation using the finite difference method. First, the radiative transfer equation may be rewritten as follows when the angle is separated into discrete and uniform $2N$ groups:

$$\mu \frac{dI_d(\tau, \mu)}{d\tau} + I_d(\tau, \mu) = \frac{1}{4N} \sum_{j=1}^{2N} P(\mu, \mu_j) I_d(\tau, \mu_j) \tag{16}$$

This equation converts the integral term of (10) into summation form with only one differential term $\frac{dI_d(\tau,\mu)}{d\tau}$. Then further divides the optical thickness τ into M groups of discrete and uniform points $\{\tau_1, \tau_2, \ldots, \tau_M\}$. Based on the forward difference method, the partial derivatives at the point τ_i can be calculated using the following equation:

$$\frac{dI_d(\tau, \mu)}{d\tau} = \frac{I_d(\tau_{i+1}, \mu) - I_d(\tau_i, \mu)}{h} \quad (0 < i < M) \tag{17}$$

Where h is the interval between each point, by this method the medium space can be divided into a two-dimensional set of space points with a size of $M * 2N$ according to distance and angle. After combining equations (16) and (17):

$$\frac{I_d(\tau_{i+1},\mu)}{h}+\left(1-\frac{1}{h}\right)I_d(\tau_i,\mu)=\frac{1}{4N}\sum_{j=1}^{2N}P(\mu,\mu_j)I_d(\tau_i,\mu_j) \tag{18}$$

The boundary conditions for equations (11) and (12) are rewritten as follows:

$$\sum_{j=1}^{N}I_d(0,\mu_j)=a\ (0<\mu_j<1) \tag{19}$$

$$\sum_{j=N+1}^{2N}I_d(d,\mu_j)=b\ (-1<\mu_j<0) \tag{20}$$

The discretized radiative transfer equations can be solved by associating the aforementioned M system of equations to obtain the luminous flux values for the $2N$ channels in the many-flux method.

4. EXPERIMENTS

4.1. Calculation of the Scattering Phase Function

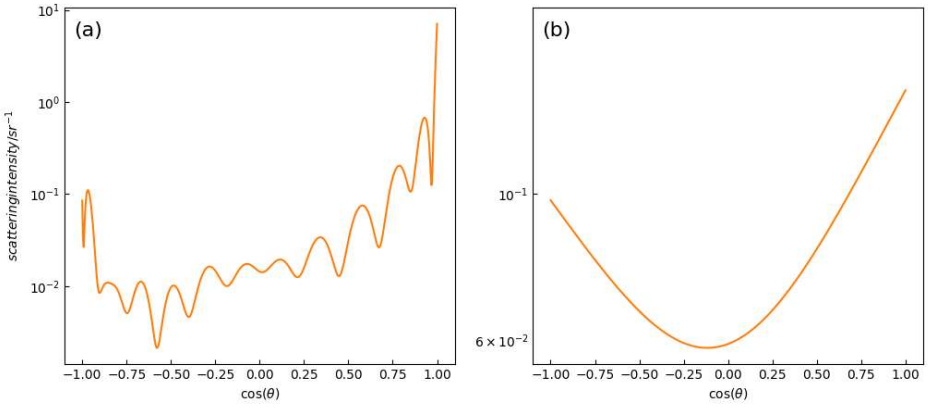

Fig. 1 Values of the phase function $p(\cos\theta)$ at the cosine of the direction of the polar angle. In Fig. 1 the relative relationship x is (a)x = 12.57 and (b)x = 0.63

In order to comprehend the variation rule of scattered light intensity with angle when the relative relationship between the particle's radius and the wavelength of the incident light is different, we change the average radius of the particle and use the software to visualize the distribution of the scattering phase function $p(\cos(\theta))$ under the wavelength of $500nm$ and the complex refractive

index m, where m is $1.5 + 0.001\mathrm{i}$. We use x to denote the relative relationship, where $x = \frac{2*\pi*r}{\lambda}$,λ are the wavelengths, r is the average radius of the particles. In Fig. 1(a), the particle radius is $1\mu m$ which is larger than the wavelength, while in Fig. 1(b), the particle radius is $0.05\mu m$ which is smaller. We may observe the difference in the intensity distribution of the scattered light by comparing the scattering phase functions in these two scenarios.

The scattering intensity exhibits clear fluctuation trends in various scattering directions when the particle radius is larger than the wavelength, as shown in the above figure. The scattering values at different angles vary greatly, but the scattering is primarily concentrated in the forward direction, with the highest scattering intensity at $\theta = 0$, which is approximately two orders of magnitude higher than that in the other directions. In contrast, when the particle radius is smaller, the magnitude of the change in the scattering intensity is relatively uniform. The vertical incident direction has the smallest scattering intensity, while the forward and backward scattering intensities are larger. At this point, the scattering distribution is more similar to Rayleigh scattering.

4.2. Analysis of the Results of the Radiative Transfer Equation

We visualize the findings of Eq. (15) at wavelengths $500nm$ to gain a better understanding of the energy distribution and transfer process during radiative transfer. Fig. 2 illustrates the radiative energy transfer between the channels. The horizontal and longitudinal coordinates represent the cosine of the polar angle corresponding to the channel of the incoming and outgoing scattering, respectively. The vertical coordinates represent the ratio of the energy transferred from the channel b to the channel a to the contribution of all channels, with the number of channels being 500.

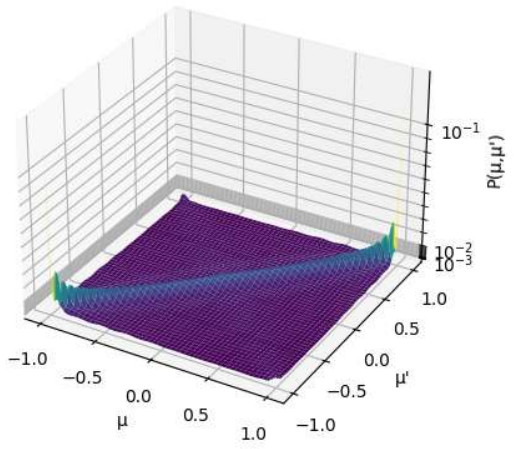

Fig. 2 Radiation intensity contribution of the phase function $P(\mu, \mu')$ passed between channels 1 and 500

Numerically simulated and visualized by the software, it can be seen in Fig. 2 that the scattering phase function is symmetric on $\mu = \mu'$ and $\mu = -\mu'$. This symmetry reflects that the process of light-particle interaction is essentially symmetric. Furthermore, in the data processed in the simulation,particle radius r = $1\mu m$, that is $x = 12.57$. This means the particle radius is larger than the wavelength. Meanwhile, the scattering intensity distribution demonstrated in the figure is overwhelmingly concentrated on $\mu = \mu'$, which indicates that the proportion of forward scattering is much larger than that of the other directions, and the intensity of the scattered light is significantly enhanced. It is in line with the general law of Mie scattering. It also shows that when the dimensions of the scattered particles are larger than the wavelength, due to the interference effect and phase

difference, the interaction between light waves and particles leads to more light being concentrated in the forward direction.

The radiative transfer equation, which was utilized to see how the radiant intensity changed as the optical thickness increased, continued to be derived and visualized based on Fig. 2. The horizontal coordinate in Fig. 3 is the cosine of the direction of the polar angle corresponding to each channel, the longitudinal coordinate is the optical thickness, and the vertical coordinate is the radiant intensity. Where the optical thickness is 1 at maximum so that the length of each differential is 0.01 and the number of channels is 100. Additionally, assuming that the a and b of Eqs. (19) and (20) are 1 and 0.9, respectively.

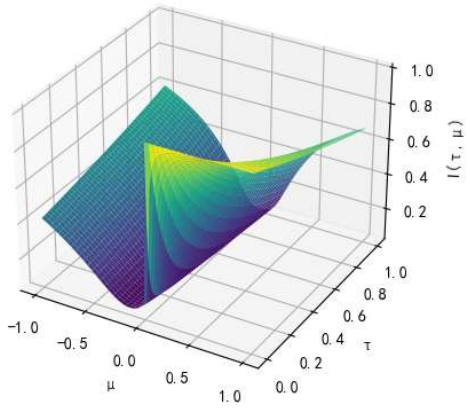

Fig. 3 Results of the radiative transfer equation for wavelengths at 500 nm

The link between radiation intensity, optical thickness, and propagation direction may be clearly analyzed in Fig. 3. According to the relationship between radiation intensity and optical thickness, the radiation intensity decreases as the optical thickness increases when the angle between the vertical incidence direction and the light's propagation direction is less than 90°, or $\mu>0$, and vice versa. Meanwhile, the relationship between radiation intensity and propagation direction shows that the radiation intensity reaches a large value at $\mu=1$ and $\mu=-1$, while in other directions it decreases sharply, with $\mu=0$ being the lowest level. The scattering percentage reaches its maximum in the direction close to $\mu = 1$, which is consistent with the Mie theory.

4.3. Substrates, Pigments, and Color Measurement Equipment

Substrate: Polypropylene (PP)

Thickness: $1.1mm$

Pigment: 0.42% high concentration red (DPP P.R.254), 0.5% high concentration green (copper phthalocyanine P.G.7)

Light source: D65 light source

Color measurement equipment: Datacolor spectrophotometer for measuring the reflectance over white and the reflectance over black.

4.4. Experimental Methods

The samples were color measured using a colorimeter in the wavelength band 400nm–700nm. The reflectance curves over white, over black, white substrate, and black substrate were measured at $10nm$ intervals and the reflectance curve over white was used as the target sample.

Determine this sample's scattering rate S and absorptivity K based on the reference hiding power and transparency measurement method.

The K-M theory and the many-flux method discussed above in this study are utilized, respectively, to forecast 31 sets of reflectance in the 400nm–700nm bands based on the known sample thickness, and compared with the target samples to verify the feasibility of the many-flux method.

4.5. Results

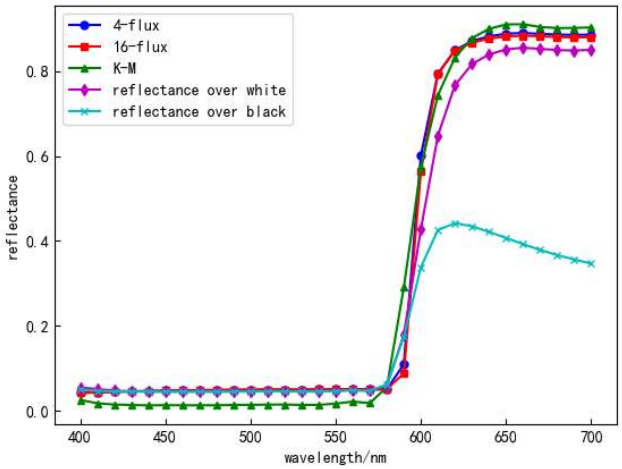

Fig. 4 Normalised reflectance predictions for 0.42% high concentration of red

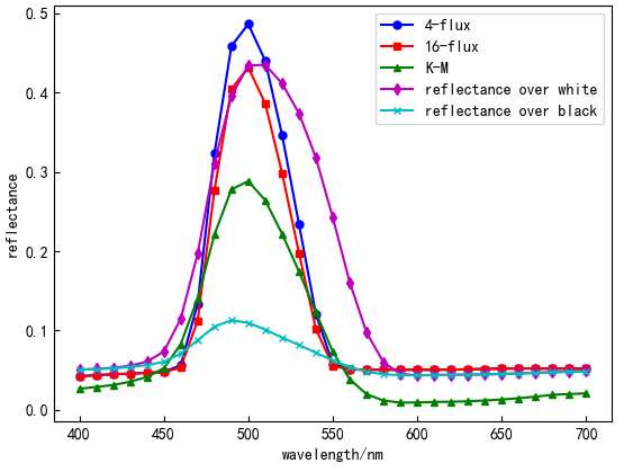

Fig. 5 Normalised reflectance predictions for 0.5% high concentration green

We can evaluate the accuracy of the many-flux method by visualizing the reflectance spectral curves of the samples under various theoretical models and then comparing them. The normalized reflectance curves of the high-concentration red and high-concentration green colorants are shown in Figs. 4 and 5, respectively. From the above two figures, it can be seen that in the visible band, the reflectance curves predicted by the K-M theory, the many-flux method, and the reflectance curves of the actual samples show similar trends overall. The errors between the reflectance curve predicted by the many-flux method and the reflectance curve over white are all smaller than those of the K-M curves. Especially when predicting higher concentrations of the green colorant, in the case where the predictions of the K-M theory are worse case, the prediction of the many-flux method still maintains

a certain accuracy. This indicates that the many-flux method has a high accuracy in predicting the reflectance of this plastic sample. Furthermore, the 16-flux method outperforms the 4-flux method in terms of accuracy as the number of channels grows.

4.6. Outlook of the Model

The color prediction model is a crucial part of the field of color matching, thus selecting an appropriate model is largely dependent on the prediction's high accuracy. However, in this experiment, we found that the model's accuracy is still poor when the scattering rate is large, which undoubtedly brings some challenges to our color-matching work. The model must thus be improved and optimized in order to further increase its accuracy and dependability:

Considering the dispersion phenomenon of light, the refractive index parameter may no longer be a constant but a variable that varies with wavelength. To further improve the accuracy of the model, wavelength-dependent refractive index data can be used to more accurately calculate the propagation path and energy distribution of light when modeling the scattering and refraction processes.

Transparency and hiding power also affect the scattering and reflection of light inside the medium, and the magnitude of the scattering coefficients can be corrected for more accurate simulations based on the actual situation such as the hiding power of the pigment.

5. SUMMARY

Relevant research is still lacking in the field of plastic color-matching modeling. To address the limitations of the traditional K-M theory, this paper uses the many-flux method and the Mie theory to simulate the energy transfer of light between multiple channels, in order to achieve an accurate portrayal of the scattering behavior of light in the medium. While also utilizing the finite difference method to simplify calculations and efficiently solve the radiative transfer equations. Following validation, the model demonstrates notable improvements in prediction accuracy, particularly when handling high concentrations of plastic colorants, it can effectively overcome the issue of distortion in traditional K-M theory prediction. The accuracy of the model is further enhanced as the number of channels increases. This research concludes by putting forward the prospect of future model improvement, pointing out that taking into account the light dispersion phenomena and the pigment hiding power would increase the model's accuracy and dependability even more. This work establishes the theoretical underpinnings for further exploration in related fields and supports scientific and intelligent pigment color matching.

REFERENCES

[1] PENG Hui,YE Huaping. Application of digital color system in textile and garment industry chain color management[J]. Textile Herald,2020(9):86-89.

[2] Huang Wenyu,Che Jiangning. Digital management of textile color - more than just color matching[J]. Textile Herald,2007(9):114-116.

[3] Xu Haisong. Principles of colour technology and its application in printing and dyeing (XVII) Part XIV Application and development of digital technology of colour in printing and dyeing industry[J]. Printing and dyeing,2006(10):41-43.

[4] Xu Yi. Digital intelligent color management in the global textile and apparel supply chain[J]. Textile Herald,2009(7):81-85.

[5] P. Kubelka. Munk F. Ein beitrag zur op tik der farbanstriche, zeits [J]. F. Techn. Physik,1931, 12:593 — 601

[6] Jiang Pengfei. Research on computer color matching theory and algorithm[D]. Zhongyuan Institute of Technology,2016.

[7] P. S. Mudgett and L. W. Richards. Multiple scattering calculations for technology[J].Applied Optics, 1971, 10(7):1485—1502

[8] Yang Yanqi. Research on plastic color matching expert system based on k-nearest neighbor algorithm integrated learning[D]. Beijing Institute of Fashion Technology,2022.DOI:10.26932/d.cnki.gbjfc.2022.000010.

[9] G. Sharma. Digital color imaging handbook[M]. CRC Press, 2003

[10] Yuan Yijun,Ren D,Hu Xiaoyong.Mie-theoretic recursive formulae for calculating the scattering phase function[J]. Journal of Light Scattering,2005,(04):366-371.DOI:10.13883/j.issn1004-5929.2005.04.011.

[11] YANG Ye, ZHANG Zhenxi, JIANG Dazong.Numerical calculation of physical quantities of Mie scattering[J]. Applied Optics,1997,(04):17-19.

[12] Defend Zhang,Mingyan Li,Weiwei Lei. Study on the analytical expression of the Conjugate Legendre Function[J]. Geodesy and Geodynamics,2015,35(04):645-648.DOI:10.14075/j.jgg.2015.04.022.

[13] LIU Shanshan, TAN Yueyue. Comparison of three phase functions for underwater optical communication channels based on Monte Carlo simulation[J]. Electronic Measurement Technology,2020,43(10):139-142.DOI:10.19651/j.cnki.emt.2004081.

[14] C.C. Li. A color prediction model based on K-M theory [D]. Jiangnan University,2008.

[15] Mehta KT, Shah HS. Simplified method of calculating Legendercoefficients for computing optical properties of pigments. Color ResAppl 1985;10:98–105.

[16] Mehta KT, Shah HS. Simplified equations to calculate Mie-theoryparameters for use in many-flux calculations for predicting the reflectance of paints films. Color Res Appl 1987;12:147–155.

[17] Mehta KT, Shah HS. Correlating parameters of Henyey–Greensteinphase function equation with size and refractive index of colorants.Appl Opt 1985;24:892–896.

[18] WANG Xiao,LIU Muhua,XU General. Research on emulsified oil spectral detection system based on dispersive polarisation[J]. Spectroscopy and Spectral Analysis,2022,42(09):2689-2693.

[19] KLOSE A D NETZ U BEUT HAN J et al. Opticaltomography using the time-independent equation of radiativetransfer-Part 1: forward model [J].Journal of QuantitativeS pectroscop y & Radiative Transfer 200272(5): 691-713.